

Optical noise correlations and beating the standard quantum limit in LIGO-II

Alessandra Buonanno and Yanbei Chen

Theoretical Astrophysics and Relativity Group,

California Institute of Technology, Pasadena, CA 91125, USA

The uncertainty principle, applied naively to the test masses of a laser interferometer gravitational wave detector, produces a *standard quantum limit* (SQL) on the interferometer's sensitivity. It has long been thought that beating this SQL would require a radical redesign of interferometers. We show that no redesign is needed at all. LIGO-II interferometers, as currently planned, can beat the SQL by as much as a factor two over a bandwidth $\Delta f \sim f$, if their thermal noise can be pushed low enough. This is due to quantum correlations between photon shot noise and radiation pressure noise, produced by the LIGO-II signal-recycling mirror.

A laser interferometer gravitational wave detector ("interferometer" for short) consists mainly of an L-shaped assemblage of four mirror-endowed test masses, suspended from seismic-isolation stacks (see Fig. 1). Laser interferometry is used to monitor changes in the relative positions of the test masses produced by gravitational waves. The uncertainty principle states that, if the relative positions are measured with high precision, then the test-mass momenta will thereby be perturbed. As time passes, the momentum perturbations will produce position uncertainties, thereby possibly masking the tiny displacements produced by gravitational waves. A detailed analysis of this process gives rise to the standard quantum limit (SQL) for interferometers: a limiting (single-sided) noise spectral density $S_h^{\text{SQL}} = 8\hbar/(m\Omega^2 L^2)$ for the dimensionless gravitational-wave (GW) signal $h(t) = \Delta L/L$ [1]. Here m is the mass of each identical test mass, L is the length of the interferometer's arms, ΔL is the time evolving difference in the arm lengths, Ω is the GW angular frequency, and \hbar is Planck's constant. This SQL is shown in Fig. 2 for the parameters of LIGO-II (the second generation interferometers in LIGO, planned to operate in ~ 2006 – 2008): $m = 30$ kg, $L = 4$ km. The "straw-man" design for LIGO-II [2], assuming (incorrectly) no correlations between photon shot noise and radiation-pressure noise, is capable of going very close and parallel to the SQL over a wide frequency band: ~ 50 Hz to ~ 200 Hz (see Fig. 2).

Vladimir Braginsky, who formulated the concept of SQL's for high-precision measurements [3], also demonstrated that it is possible to circumvent SQL's by changing the designs of one's instruments [3], [4]. Since the 1970s, it has been thought that for GW interferometers the redesign would have to be major — e.g., injecting squeezed vacuum into an interferometer's dark port [5] and/or introducing 4km-long filter cavities into the interferometer's output port, as has recently been proposed for LIGO-III [6] to implement frequency-dependent homodyne detection [7].

In this paper we show that, in fact, no redesign is needed at all. With their currently planned design, LIGO-II interferometers can beat the SQL by modest

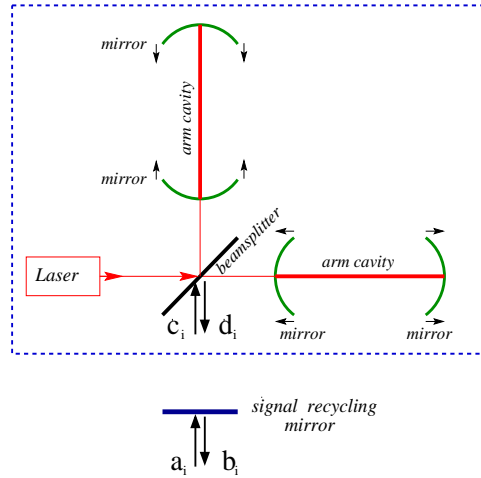


FIG. 1. Schematic view of a LIGO-II signal-recycling (SR) interferometer. The interior of the dashed box is a conventional LIGO-I interferometer; c_i and d_i are the input and output fields at the beam splitter's dark port; a_i and b_i are the full system's vacuum input and signal output. The arrows indicate gravity-wave-induced mirror displacements.

amounts (see, e.g., noise curves b_1 and b_2 in Fig. 2), if all sources of thermal noise can also be pushed below the SQL. The thermal noise is a formidable problem. For current LIGO-II designs, estimates place its dominant, thermoelastic component at about the SQL [8], and much R&D will go into trying to push it downward. This topic is beyond the scope of our paper.

The keys to LIGO-II beating the SQL are readily explained. As is well known, there are two aspects of the uncertainty principle: (i) the quantum mechanics of the test-mass wave function (the narrower it is peaked due to an accurate position measurement, the greater the uncertainty in the momentum), and (ii) the Heisenberg-microscope-like influence of the laser light used to measure the position (the higher the laser power I_0 , the lower the photon shot noise and thus the more accurate the measurement of position, but also the larger the fluctuations in the radiation pressure acting on the test masses and hence the larger the momentum perturbations). Recently Braginsky and colleagues [9], building on earlier work of Braginsky and Khalili [4], have shown that the

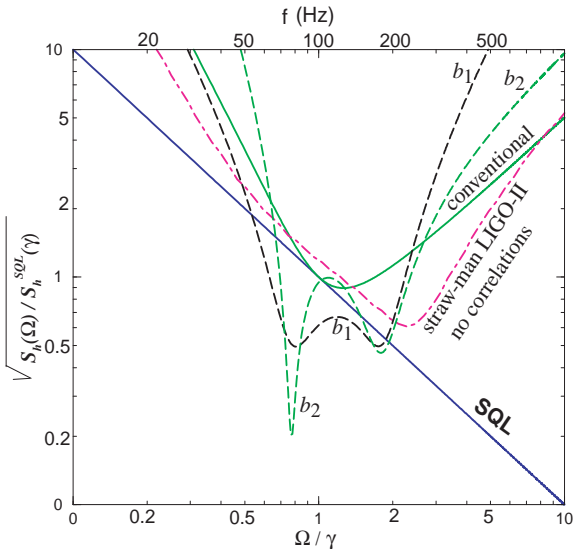


FIG. 2. Log-log plot of $\sqrt{S_h(\Omega)/S_h^{\text{SQL}}(\gamma)}$ versus Ω/γ for the quadratures b_1 ($\zeta = \pi/2$) and b_2 ($\zeta = 0$) with $\rho = 0.9$, $\phi = \pi/2 - 0.47$ and $I_0 = I_{\text{SQL}}$, for the SQL, for a conventional interferometer with $I_0 = I_{\text{SQL}}$, and for a straw-man LIGO-II design [2] with shot-noise / radiation-pressure correlations incorrectly omitted. For LIGO-II, $\gamma = 2\pi \times 100 \text{ Hz}$ (top axis) and $\sqrt{S_h^{\text{SQL}}(\gamma)} = 2 \times 10^{-24} \text{ Hz}^{-1/2}$. These curves do not include seismic and thermal noises; for LIGO-II the latter is expected to be approximately the same as the SQL [8].

test-mass wave-function aspect of the uncertainty principle is irrelevant to the operation of a GW interferometer. The reason, in brief, is that the interferometer does *not* measure the relative test-mass positions; it only monitors classical-force-induced changes in the relative positions, and those changes, in the LIGO frequency band, manage to avoid any contamination at all by the details of the test-mass wave functions. As a result, *the light is the only enforcer of the SQL*.

As we demonstrate below, as long as there are no correlations between the light's shot noise and its radiation-pressure-fluctuation noise, the light firmly enforces the SQL. This is the case for "conventional interferometers", i.e. for interferometers that have no signal-recycling mirror on the output port (the type of interferometer used, e.g., in LIGO-I). However, as we shall show, the signal-recycling (SR) mirror (which is being planned for LIGO-II as a tool to reshape the noise curve) produces shot-noise / back-action-noise correlations, and *these correlations break the light's ability to enforce the SQL*. The remainder of this paper is devoted to explaining these claims. The full details will be published elsewhere [10].

Kimble et al. have recently derived the input-output relations for a conventional interferometer [6] using the Caves-Schumaker two-photon formalism [11]. The full electric field, in the Heisenberg picture, at the output (dark) port, i.e. soon after the beamsplitter (see Fig. 1), reads:

$$E(t) = \sqrt{\frac{4\pi\hbar\omega_0}{\mathcal{A}c}} \left[\cos(\omega_0 t) \int_0^\infty (d_1 e^{-i\Omega t} + d_1^\dagger e^{i\Omega t}) \frac{d\Omega}{2\pi} \right. \\ \left. + \sin(\omega_0 t) \int_0^\infty (d_2 e^{-i\Omega t} + d_2^\dagger e^{i\Omega t}) \frac{d\Omega}{2\pi} \right], \quad (1)$$

where d_1 and d_2 are the two output quadratures (see Fig. 1), ω_0 is the carrier angular frequency, \mathcal{A} is the effective cross sectional area of the laser beam and c is the velocity of light. Indicating by c_1 and c_2 the two input quadratures at the dark port, the input-output relations, at side-band (gravity-wave) angular frequency Ω , are [6]:

$$d_1 = c_1 e^{2i\beta}, \quad d_2 = (c_2 - \mathcal{K}c_1) e^{2i\beta} + \frac{h\sqrt{2\mathcal{K}}e^{i\beta}}{h_{\text{SQL}}}, \quad (2)$$

where $2\beta = 2 \arctan \Omega/\gamma$ is the net phase gained by the field at sideband frequency Ω while in the arm cavity, $\gamma = Tc/4L$ is the half bandwidth of the arm cavity (T is the power transmissivity of the input mirrors); h is the Fourier transform of the GW field, and $h_{\text{SQL}} \equiv \sqrt{S_h^{\text{SQL}}}$ is the SQL for GW detection. The quantity $\mathcal{K} = 2(I_0/I_{\text{SQL}})\gamma^4/(\Omega^2(\gamma^2 + \Omega^2))$ in Eq. (1) is the effective coupling constant which relates the motion of the test mass to the output signal. Finally, I_0 is the input laser power, while $I_{\text{SQL}} = mL^2\gamma^4/(4\omega_0)$ is the laser power needed by a conventional interferometer to reach the SQL. We indicate by l the length of the SR cavity and we introduce two variables: $\phi \equiv [\omega_0 l/c]_{\text{mod } 2\pi}$, the phase gained by the carrier while traveling one way in the SR cavity, and $\Phi \equiv [\Omega l/c]_{\text{mod } 2\pi}$, the additional phase gained by the sideband.

Propagating the electric field (1) down to the SR mirror and introducing the input and output quadratures a_i and b_i ($i = 1, 2$) for the entire SR interferometer (Fig. 1), we obtain the final input-output relations [10]:

$$\begin{pmatrix} b_1 \\ b_2 \end{pmatrix} = \frac{1}{M} \left[\begin{pmatrix} C_{11} & C_{12} \\ C_{21} & C_{22} \end{pmatrix} \begin{pmatrix} a_1 \\ a_2 \end{pmatrix} + \frac{h\sqrt{2\mathcal{K}}\tau}{h_{\text{SQL}}} \begin{pmatrix} D_1 \\ D_2 \end{pmatrix} \right], \quad (3)$$

where, to ease the notation, we have defined:

$$M = e^{-2i(\beta+\Phi)} + \rho^2 e^{2i(\beta+\Phi)} - 2\rho \left[\cos 2\phi + \frac{\mathcal{K}}{2} \sin 2\phi \right], \\ C_{11} = C_{22} = (1 + \rho^2) \left[\cos 2\phi + \frac{\mathcal{K}}{2} \sin 2\phi \right] \\ - 2\rho \cos 2(\beta + \Phi), \\ C_{12} = -\tau^2 [\sin 2\phi + \mathcal{K} \sin^2 \phi], \\ C_{21} = +\tau^2 [\sin 2\phi - \mathcal{K} \cos^2 \phi], \\ D_1 = - \left[e^{-i(\beta+\Phi)} + \rho e^{i(\beta+\Phi)} \right] \sin \phi, \\ D_2 = - \left[-e^{-i(\beta+\Phi)} + \rho e^{i(\beta+\Phi)} \right] \cos \phi. \quad (4)$$

In the above equations ρ and τ are the amplitude reflectivity and transmissivity of the SR mirror, respectively. For a lossless SR mirror: $\tau^2 + \rho^2 = 1$. Because a_i, a_i^\dagger in Eq. (3) represent a free field, they satisfy the usual commutation relations for quadratures with $\Omega \ll \omega_0$ [11]: $[a_1, a_{2'}^\dagger] = -[a_2, a_{1'}^\dagger] = 2\pi i\delta(\Omega - \Omega')$, $[a_1, a_{1'}^\dagger] = [a_1, a_{1'}^\dagger] = [a_2, a_{2'}^\dagger] = [a_2, a_{2'}^\dagger] = 0$, where $a_{i'}$ stands for $a_i(\Omega')$. A straightforward calculation confirms that the quadratures b_i, b_i^\dagger also satisfy the standard commutation relations. Let us observe that, both the quadratures b_1 and b_2 in Eq. (3) contain the GW signal h and it is not possible to put the signal into just one of the quadratures through a transformation that preserves the commutation relations of b_1 and b_2 [10].

Henceforth, we limit our analysis to $\Phi = 0$, which corresponds to a SR cavity much shorter than the arm cavities, e.g., $l \simeq 10$ m. We assume for simplicity that there is no radio-frequency modulation/demodulation of the carrier and the signal [2]; instead some frequency-independent quadrature $b_\zeta = b_1 \sin \zeta + b_2 \cos \zeta$ is measured via homodyne detection. Using homodyne detection, the noise is calculated as follows [6]. We define $h_n(\Omega) \equiv \Delta b_\zeta h_{\text{SQL}} M / [\sqrt{2\mathcal{K}}\tau(D_1 \sin \zeta + D_2 \cos \zeta)]$, where Δb_ζ is the noise part of b_ζ , and then the (single-sided) spectral density $S_h(f)$ of h_n , with $f = \Omega/2\pi$, can be computed by the formula: $2\pi\delta(\Omega - \Omega')S_h(f) = \langle h_n(\Omega)h_n^\dagger(\Omega') + h_n^\dagger(\Omega')h_n(\Omega) \rangle$. Assuming that the input is in its vacuum state, we find [10] that the noise spectral density can be written in the simple form (note that $C_{ij} \in \Re$):

$$S_h = \frac{h_{\text{SQL}}^2}{2\mathcal{K}} \frac{1}{\tau^2 |D_1 \sin \zeta + D_2 \cos \zeta|^2} \times \left[(C_{11} \sin \zeta + C_{21} \cos \zeta)^2 + (C_{12} \sin \zeta + C_{22} \cos \zeta)^2 \right]. \quad (5)$$

Fig. 2 shows this $S_h(f)$ for the two quadratures b_1 (i.e. $\zeta = \pi/2$) and b_2 ($\zeta = 0$), with (for definiteness) $\rho = 0.9$, $\phi = \pi/2 - 0.47$ and $I_0 = I_{\text{SQL}}$. Also shown for comparison are the SQL, and $S_h(f)$ for a straw-man LIGO-II design when the shot-noise/radiation-pressure correlations are (incorrectly) ignored [2], and for a conventional interferometer with $I_0 = I_{\text{SQL}}$. The sensitivity curves for the two quadratures go substantially below the SQL and show an interesting resonance structure. To explain the resonant frequencies in the case of a highly-reflecting SR mirror, we have found it convenient to investigate the *free* oscillation modes of the entire interferometer. By *free* we mean no GW signals [$h(\Omega) = 0$] and perfect reflectivity for the SR mirror ($\rho = 1$). The free-oscillation frequencies satisfy the relation [10]: $\cos 2\beta = \cos 2\phi + \mathcal{K} \sin \phi \cos \phi$, which can be solved to give $\Omega_{\text{res.}}^2 / \gamma^2 = [\tan^2 \phi \pm \sqrt{\tan^4 \phi - 4I_0/I_{\text{SQL}} \tan \phi}] / 2$, which agrees quite accurately with the frequencies of the valleys in the noise dashed curves of Fig. 2.

To give a first rough idea of the performances a SR in-

terferometer with homodyne detection can reach *if thermal noise can be made negligible*, we have estimated the signal-to-noise ratio $(S/N)^2 = 4 \int_0^\infty |h(f)|^2 / S_h(f) df$ [1] for gravitational waves from binary systems made of black holes and/or neutron stars. Using the Newtonian, quadrupole approximation for which the waveform's Fourier transform is $|h(f)|^2 \propto f^{-7/3}$, and introducing in the above integral a lower cutoff due to seismic noise at $\Omega_s = 0.1\gamma$ ($f_s \simeq 10$ Hz), we get for the parameters used in Fig. 2: $(S/N)_1 / (S/N)_{\text{conv.}} \simeq 1.83$ and $(S/N)_2 / (S/N)_{\text{conv.}} \simeq 1.98$. These numbers refer to the first and second quadratures, respectively. A more thorough investigation of signal-to-noise ratio for inspiraling binaries will be published elsewhere [10].

We now briefly discuss how optical losses affect the noise in a SR interferometer. We have computed [10] the influence of losses using (i) the lossy input-output relations [analog of Eq. (2)] for a conventional interferometer [boxed part of Fig. 1] as derived in [6], and (ii) an analogous treatment of losses in the SR cavity. We find that for loss levels expected in LIGO-II [2], the optical losses have only a small influence on the noise curves of Fig. 2; primarily, they just smooth out the deep resonant valleys. More specifically, for (i) the physical parameters used in Fig. 2, (ii) a net fractional photon loss of 1% in the arm cavities and 2% in each round trip in the SR cavity, and (iii) a photodetector efficiency of 90%, we find a fractional loss in S/N for inspiraling binaries of 8% and 21%, for the first and second quadratures, respectively.

In the last part of this letter we discuss the crucial role played by the shot-noise / radiation-pressure correlations, present in the LIGO-II's noise spectral density (5), in beating the SQL. Our analysis is based on the general formulation of linear quantum measurement theory developed in [4] and assumes the results obtained in [9]. We find it convenient to address the problem in terms of an *effective* * output noise field \mathcal{Z} and an *effective* back-action force \mathcal{F} . Quite generically [4,10], we can rewrite the output \mathcal{O} of the whole optical system as: $\mathcal{O} = \mathcal{Z} + \mathcal{R}_{xx} \mathcal{F} + Lh$. Here by output we mean one of the two quadratures b_1, b_2 or a combination of them, e.g., b_ζ (modulo a normalization factor). \mathcal{R}_{xx} in the above equation is the susceptibility of the asymmetric mode of motion of the four mirrors [4], given by $\mathcal{R}_{xx}(\Omega) = -4/(m\Omega^2)$. The noise spectral density, written in terms of the effective operators \mathcal{Z} and \mathcal{F} , reads [4]:

* We refer to \mathcal{Z} and \mathcal{F} as effective because we have shown [10] that for a SR interferometer the *real* force acting on the test masses is a combination of these effective fields. When the shot noise and radiation-pressure-noise are correlated, the real force does not commute with itself at different times [10], which makes the analysis in terms of real quantities more complicated than in terms of the effective ones.

$$S_h = \frac{1}{L^2} \{ S_{ZZ} + 2\mathcal{R}_{xx} \Re[S_{\mathcal{F}\mathcal{Z}}] + \mathcal{R}_{xx}^2 S_{\mathcal{F}\mathcal{F}} \}, \quad (6)$$

where the (one-sided) spectral density of two operators is defined by $2\pi\delta(\Omega - \Omega') S_{AB}(\Omega) = \langle \mathcal{A}(\Omega)\mathcal{B}^\dagger(\Omega') + \mathcal{B}^\dagger(\Omega')\mathcal{A}(\Omega) \rangle$. In Eq. (6) the terms containing S_{ZZ} , $S_{\mathcal{F}\mathcal{F}}$ and $\Re[S_{\mathcal{F}\mathcal{Z}}]$ should be identified as effective shot noise, back-action noise and a term proportional to the effective correlation between the two noises [4]. From the definition of the spectral density, one can derive [4,10] the following uncertainty relation for the (one-sided) spectral densities and cross correlations of \mathcal{Z} and \mathcal{F} :

$$S_{ZZ} S_{\mathcal{F}\mathcal{F}} - S_{Z\mathcal{F}} S_{\mathcal{F}Z} \geq \hbar^2. \quad (7)$$

It turns out that Eq. (7) does not impose in general a lower bound on the noise spectral density (6). However, in a very important type of interferometer it does, namely for interferometers with uncorrelated shot noise and back-action noise, e.g., a LIGO-I type conventional interferometer. In this case $S_{Z\mathcal{F}} = 0 = S_{\mathcal{F}Z}$ [6] and inserting the vanishing correlations into Eqs. (6), (7), one easily finds that $S_h \geq S_h^{\text{SQL}}$. From this it follows that to beat the SQL one must create correlations between shot noise and back-action noise.

Let us derive these correlations for a SR interferometer. For simplicity we restrict ourselves to the two quadratures separately. By identifying, in the output (see Eq. (3) properly normalized) the terms proportional to $1/\sqrt{\mathcal{K}}$ as effective shot noise and those proportional to $\sqrt{\mathcal{K}}$ as effective back-action noise, we get the effective field operators \mathcal{Z}_1 , \mathcal{Z}_2 , \mathcal{F}_1 and \mathcal{F}_2 [10]. Evaluating the spectral densities of these operators we obtain the following expressions for the correlations:

$$\begin{aligned} S_{\mathcal{F}_1\mathcal{Z}_1} &= S_{\mathcal{Z}_1\mathcal{F}_1} = \\ &= -\frac{\hbar [(-1 + \rho^2)^2 - 2\rho(1 + \rho^2) \cos 2\beta + 4\rho^2 \cos 2\phi] \cot \phi}{(1 - \rho^2)(1 + \rho^2 + 2\rho \cos 2\beta)}, \\ S_{\mathcal{F}_2\mathcal{Z}_2} &= S_{\mathcal{Z}_2\mathcal{F}_2} = \\ &= \frac{\hbar [(-1 + \rho^2)^2 + 2\rho(1 + \rho^2) \cos 2\beta - 4\rho^2 \cos 2\phi] \tan \phi}{(1 - \rho^2)(1 + \rho^2 - 2\rho \cos 2\beta)}. \end{aligned} \quad (8)$$

These correlations depend on the sideband angular frequency Ω and are generically different from zero. However, there are two (extreme) cases, already investigated in the literature within a semi-classical approach [12], for which the correlations are zero: (i) the extreme SR configuration where the detuning frequency is zero (i.e. $\phi = 0$) and the GW signal appears only in b_2 ; (ii) the extreme resonant sideband extraction configuration where $\phi = \pi/2$ and the signal is solely in b_1 .

In conclusion, our analysis has demonstrated the importance of using fully quantum techniques to analyze SR interferometers, e.g. LIGO II. The quantum formalism reveals the shot-noise / radiation-pressure correlations

(produced by the SR cavity). These correlations break the light's ability to enforce the SQL and allow it to be beaten; they also change the shapes of noise curves even when the SQL is not being beaten (e.g., in the presence of large thermal noise). It is now important to identify the best SR configuration, i.e. the choice of the physical parameters I_0 , ϕ , ρ , ζ , and the readout scheme (heterodyne or modulation/demodulation) that optimizes the S/N for inspiraling binaries and other astrophysical GW sources.

The authors wish to thank K.S. Thorne for having introduced us to QND theory, for his constant encouragement and for very fruitful discussions and comments. It is also a pleasure to thank V.B. Braginsky, Y. Levin and K.A. Strain for very helpful discussions and comments. This research was supported in part by NSF grant PHY-9900776 and in part (for AB) by the Richard C. Tolman Fellowship.

- [1] K.S. Thorne, in *Three Hundred Years of Gravitation*, eds. S.W. Hawking and W. Israel, (Cambridge University Press, Cambridge, 1987), p. 330 and references therein.
- [2] E. Gustafson, D. Shoemaker, K. Strain and R. Weiss, *LSC White paper on Detector Research and Development*, LIGO Document Number T990080-00-D (Caltech/MIT, 11 September 1999).
- [3] V.B. Braginsky, Sov. Phys. JETP **26** (1968) 831; V.B. Braginsky and Yu.I. Vorontsov, Sov. Phys. Uspekhi **17** (1975) 644; V.B. Braginsky, Yu.I. Vorontsov and F.Ya. Khalili, Sov. Phys. JETP **46** (1977) 705.
- [4] V.B. Braginsky and F.Y. Khalili, *Quantum measurement*, ed. K.S. Thorne (Cambridge University Press, Cambridge, 1992).
- [5] C.M. Caves, Phys. Rev. **D 23** (1981) 1693; W. G. Unruh, in *Quantum Optics, Experimental Gravitation, and Measurement Theory*, eds. P. Meystre and M.O. Scully (Plenum, 1982), p. 647.
- [6] H.J. Kimble, Y. Levin, A.B. Matsko, K.S. Thorne and S.P. Vyatchanin, [gr-qc/0008026].
- [7] S.P. Vyatchanin and A.B. Matsko, JETP **77** (1993) 218; S.P. Vyatchanin and E.A. Zubova, Phys. Lett. **A 203** (1995) 269; S.P. Vyatchanin and A.B. Matsko, JETP **82** (1996) 1007; ibid. JETP **83** (1996) 690; S.P. Vyatchanin, Phys. Lett. **A 239** (1998) 201.
- [8] V.B. Braginsky, M.L. Gorodetsky and S.P. Vyatchanin, Phys. Lett. **A 264** (1999) 1; Y.T. Liu and K.S. Thorne, [gr-qc/0002055].
- [9] V.B. Braginsky, M.L. Gorodetsky, F.Y. Khalili, A.B. Matsko, K.S. Thorne, S.P. Vyatchanin, in preparation.
- [10] A. Buonanno and Y. Chen, in preparation.
- [11] C.M. Caves and B.L. Schumaker, Phys. Rev. **A 31** (1985) 3068; B.L. Schumaker and C.M. Caves, Phys. Rev. **A 31** (1985) 3093.
- [12] B.J. Meers, Phys. Rev. **D 38** (1988) 2317; J. Mizuno, K.A. Strain, P.G. Nelson, J.M. Chen, R. Schilling, A. Rudiger, W. Winkler and K. Danzmann, Phys. Lett. **A 175** (1993) 273; J. Mizuno, PhD thesis (1995).